

Kinetics and mechanisms of the reactions of benzoyl derivatives of nucleophiles: dependence of the solvation requirement of the reaction on the structures of the nucleophile and the acyl group[†]

Omar A. El Seoud,^{1*} Monica Ferreira,² Wagner A. Rodrigues¹ and Marie-Françoise Ruasse³

¹Instituto de Química, Universidade de São Paulo, C.P. 26077, 05513-970 São Paulo, S.P., Brazil

²Functional Chemicals Division, Clariant SA, São Paulo, Brazil

³Institut de Topologie et de Dynamiques des Systèmes, Université de Paris VII–CNRS, 1 Rue Guy de la Brosse, F-75005 Paris, France

Received 30 January 2004; revised 19 April 2004; accepted 11 May 2004

ABSTRACT: The reactions of two series of benzoyl derivatives of nucleophiles were investigated and the results were compared with those for *N*-benzoylimidazole. The general structure is ArCO–Nu, where Ar = X–C₆H₄– and/or X₂–C₆H₃–; X = 4-Me, H, 4-Cl, 4-CN, 4-NO₂ and X₂ = 3,5-dinitro; Nu = iodosobenzoate, ArCO–Iba, and phosphate dianion, ArCO–Phos. Catalytic rate constants, kinetic solvent isotope effects, kinetic substituent effects (Hammett equation) and the dependence of ΔH^\ddagger and ΔS^\ddagger on σ_X were determined. For ArCO–Iba, the hydrolysis occurs via two pathways, uncatalyzed ($k_{\text{H}_2\text{O}}$) and specific base-catalyzed (k_{OH^-}) water attack on the iodine atom of the iodosobenzoate ring. This conclusion is based on theoretical calculations of the partial charges on ArCO–Iba, and the small ρ values calculated at 25 °C, –0.22 and 0.92 for $k_{\text{H}_2\text{O}}$ and k_{OH^-} , respectively. The data for the reaction of ArCO–Phos are consistent with a dissociative transition state, leading to elimination of the metaphosphate monoanion (PO₃[–]). The dependence of the mechanistic pathway on the nucleophile is discussed. Two results are relevant to the reactions of ArCO–Iba: (i) moderate to large substituent effects on the activation entropies suggest that solvation of the leaving benzoate anion and desolvation of the entering nucleophile contribute to the OH[–]-mediated reaction; (ii) the negative and positive signs of ΔS^\ddagger indicate large differences in solvation of the transition states of the $k_{\text{H}_2\text{O}}$ and k_{OH^-} pathways. For the spontaneous decomposition of ArCO–Phos, sizeable substituent effects on both ΔH^\ddagger and ΔS^\ddagger were observed. This shows the contribution of solvation of the leaving benzoate and substituent-induced shift of the structure of the transition state. Copyright © 2004 John Wiley & Sons, Ltd.

KEYWORDS: benzoyl phosphates; decomposition; benzoyl iodosobenzoates; hydrolysis; acyl derivatives of nucleophiles; reaction mechanisms

INTRODUCTION

Studies of the mechanistic details of acyl-transfer reactions have contributed a great deal to our understanding of several problems of central importance in chemistry and biochemistry, including effects of structure on reactivity and the mechanism of action of hydrolytic enzymes.^{1–3} In addition to uncatalyzed water addition, $k_{\text{H}_2\text{O}}$, these reactions may be subject to specific, e.g. k_{OH^-} , general, k_{GB} , and nucleophilic catalysis. In ester hydrolysis, the last pathway leads to the formation of an intermediate, an acyl derivative of the nucleophile, whose

formation and subsequent decomposition have been the subject of intense research, because of its relevance to mechanism of chemical and enzymatic catalysis.^{4–9}

Much attention has been devoted to the mechanism of formation of RCO–Nu and/or ArCO–Nu (concerted or stepwise; R = alkyl moiety) than to its subsequent decomposition,^{9b,d} although the latter step is important, since it determines the catalyst turnover. Mechanistic studies of the decomposition of R- and/or ArCO–Nu have been carried out mainly on enzymes, or enzyme models, in order to understand acyl transfers between nucleophiles. It is not surprising, therefore, that the investigated intermediates were mainly R- and/or ArCO–Imz and R- and/or ArCO–Phos (Nu = imidazole and phosphate, respectively) since these two nucleophiles play a major role in biochemical reactions.^{5–10} These studies have indicated that acyl derivatives of nucleophiles may decompose by a variety of mechanisms, depending on the structures of the acyl moiety, the nucleophile and reaction conditions. Figure 1 depicts

*Correspondence to: O. A. El Seoud, Instituto de Química, Universidade de São Paulo, C.P. 26077, 05513-970 São Paulo, S.P., Brazil.
E-mail: elseoud@iq.usp.br

[†]Selected article presented at the Seventh Latin American Conference on Physical Organic Chemistry (CLAFQO-7), 21–26 September 2003, Florianópolis, Brazil.

Contract/grant sponsor: São Paulo State Research Foundation, FAPESP.

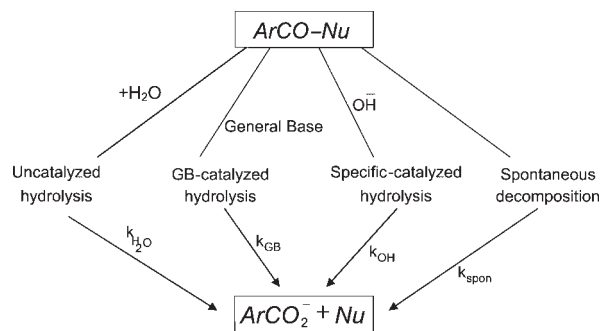


Figure 1. Mechanistic pathways for the decomposition of a typical acyl derivative of nucleophile, ArCO-Nu , in basic media. For simplicity, we do not show the negative sign of the hydroxide ion in k_{OH}

the main pathways for the decomposition reactions of ArCO-Nu in basic media, where k_{spon} refers to spontaneous decomposition.

Hydrolysis of ArCO-Imz is well documented; the reaction is subjected to specific and general acid–base catalysis.^{7,8a} The reactions of dianionic ArCO-Phos and of phosphate monoester dianions appear to proceed by a dissociative mechanism, via a metaphosphate-like transition state.^{9,10} It is not possible, *a priori*, to predict the favored catalytic mechanism for nucleophiles other than Phos , Imz or amines, although this knowledge adds to our understanding of catalysis in chemistry and enzymology.

We have studied the hydrolysis of phenyl benzoates, substituted in the acyl (by X) and in the leaving phenol (by Y).⁸ The three buffers employed were Imz , the *o*-iodosobenzoate anion, Iba , and monohydrogenphosphate dianion, Phos . Our interest in these buffers is due to the following reasons: (i) although their $\text{p}K_{\text{a}}$ values are similar, namely 7.53, 7.05 and 7.20 for Iba , Imz and Phos , respectively, their catalytic efficiencies (in ester hydrolysis) are very different, $\text{IBA} > \text{Imz} \gg \text{Phos}$;^{8d} (ii) Iba is a powerful nucleophile, with potential use in large-scale decontamination of toxic chemical substances and wastes, including phosphorelated pesticides and chemical warfare agents;^{11–13} (iii) to our knowledge, there is no

information on the kinetics and mechanism of the hydrolysis of ArCO-Iba .

The general reaction scheme is given in Fig. 2.

Catalytic rate constants, activation parameters, kinetic solvent isotope effects (KSIE) and Hammett ρ values have been determined for the formation of ArCO-Nu and for the hydrolysis of ArCO-Imz ⁸ (formally, these ρ values are equivalent to Brønsted $\beta_{\text{leaving group}}$, since σ is obtained from the effect of X on the $\text{p}K_{\text{a}}$ of benzoic acid, the leaving group in our reactions; nevertheless, we discuss substituent effects in terms of ρ , rather than $\beta_{\text{leaving group}}$, since the latter is not very informative in the absence of the corresponding $\beta_{\text{entering nucleophile}}$). We now address the kinetics and mechanism of reactions of the two other intermediates, namely ArCO-Iba and ArCO-Phos , where $\text{Ar} = X\text{-C}_6\text{H}_4\text{-}$ and/or $X_2\text{-C}_6\text{H}_3\text{-}$; $X = 4\text{-Me}$, H , 4-Cl , 4-CN , 4-NO_2 and $X_2 = 3,5\text{-dinitro}$. We anticipated that ArCO-Phos dianion may decompose spontaneously, as shown previously for the dianions of acetyl phosphate and phosphate monoesters.^{5b,10} No prediction was made regarding the hydrolysis of ArCO-Iba , as the reaction is open to different pathways shown in Fig. 1.

We show that the hydrolysis of ArCO-Iba proceeds by the $k_{\text{H}_2\text{O}}$ and k_{OH} pathways, but do not show measurable k_{GB} . The behavior of ArCO-Phos agrees with our prediction (spontaneous decomposition). A comparison of the above-mentioned quantities, i.e. ρ , KSIE and activation parameters, for the three intermediates indicates that (i) ρ does not depend much on the mechanism of catalysis, (ii) substituent effects on the activation parameters are more characteristic of each of the catalytic pathways and (iii) solvation of the appropriate species (entering nucleophile and leaving group) plays an important role, independent of the catalysis mechanism.

EXPERIMENTAL

The solvents and other reagents were purchased from Aldrich and were purified by standard procedures.¹⁴ The

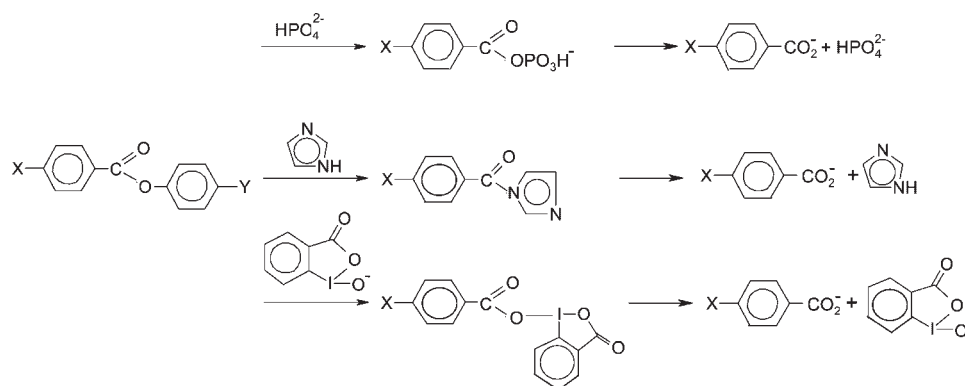


Figure 2. Complete reaction scheme for the hydrolysis of benzoate esters, catalyzed by phosphate, imidazole and *o*-iodosobenzoate buffers

purity of all solid reagents was checked by measuring their melting-points. Iba was available from a previous study.^{8c}

Synthesis of ArCO-Iba and ArCO-Phos

Acyl chlorides. These were prepared by refluxing the appropriate benzoic acid with excess purified thionyl chloride (molar ratio 1:4, bath temperature ca 130 °C) for 6 h, followed by removal of SOCl₂ and distillation of the acyl chloride. PCl₅ was employed for the preparation of 3,5-dichlorobenzoyl chloride, as given elsewhere,^{15a} and was purified by crystallization from a mixture of CCl₄ and light petroleum (b.p. 30–60 °C). The b.p.s and m.p.s of the acyl chlorides were in agreement with the values published elsewhere.¹⁵

ArCO-Iba. To a solution of the acyl chloride (2 mmol) in CH₂Cl₂ (25 ml) were added 25 ml of an aqueous solution containing Iba (2 mmol), NaOH (2 mmol) and 0.02 g of tetra(*n*-butyl)ammonium hydrogensulfate. The two-phase mixture was vigorously stirred at room temperature, until a solid compound separates at the CH₂Cl₂/water interface. The reaction time was found to depend on the nature of X, ranging from 1 min for X = NO₂ to 3 min for X = CH₃. The solid formed was quickly filtered, washed with cold CH₂Cl₂ and dried over P₄O₁₀ under reduced pressure. The products gave satisfactory elemental analyses (Perkin-Elmer Model 2400 CHN, Elemental Analysis Laboratory, University of São Paulo) and the expected IR bands (KBr pellets, Perkin-Elmer 1750 FTIR), as shown in Table 1.

ArCO-Phos. These were synthesized *in situ* by reacting the appropriate acyl chloride with (*n*-C₄H₉)₄N⁺ H₂PO₄[−] in dry acetonitrile. The organic phosphate salt was prepared by reacting 2 ml of 85% orthophosphoric acid with 19.5 ml of a 40% aqueous solution of (*n*-C₄H₉)₄N⁺ OH[−], followed by adjustment of the pH to 4.3 (with H₃PO₄) and evaporation of water. The hygroscopic product was dried over P₄O₁₀ under reduced pressure. Calculated for C₁₆H₃₈NPO₄: C, 56.66; H, 11.20; N, 4.12. Found: C, 56.38; H, 11.08; N, 4.12%.

The following example shows the completeness of the reaction between 4-nitrobenzoyl chloride and (*n*-C₄H₉)₄N⁺ H₂PO₄[−]. A solution containing 0.03 mol of the acyl chloride and 0.0315 mol of the organic phosphate salt was mixed and left to react at room temperature. The IR spectrum was periodically scanned in order to determine the reaction progress. It showed the complete disappearance of the acyl chloride $\nu_{C=O}$ (ca 1760 cm^{−1}), with concomitant appearance of the mixed anhydride $\nu_{C=O}$ (ca 1739 cm^{−1}).¹⁶

Kinetic measurements

Reaction kinetics were studied with Zeiss PM6KS, Beckman DU-70 UV–visible or Applied Photophysics stopped-flow spectrophotometers; the last is provided with syringes of unequal volumes. These instruments are fitted with thermostated cell holders whose temperature was kept constant to within ± 0.05 °C. The conditions employed are shown in Table 2. For comparison, we have also included the conditions previously employed in the hydrolysis of ArCO-Imz.^{8b}

Table 1. Elemental analysis and IR frequencies of ArCO-Iba

X	M.p. (°C)	Calculated (%)			Found (%)			IR frequencies (cm ^{−1})
		C	H	N	C	H	N	
4-CH ₃	198–199	47.41	2.90		47.05	2.85		33101 (ν_{C-H}); 1685 ($\nu_{C=O}$); 1631 ($\nu_{C=O}$)
H	192–193	45.68	2.46		45.42	2.36		3100 (ν_{C-H}); 1689 ($\nu_{C=O}$); 1633 ($\nu_{C=O}$)
4-Cl	199–200	41.77	2.00		41.55	1.92		3109 (ν_{C-H}); 1679 ($\nu_{C=O}$); 1642 ($\nu_{C=O}$)
4-CN	205–206	45.83	2.05	3.58	45.64	2.00	3.16	3084 (ν_{C-H}); 2229 ($\nu_{C\equiv N}$); 1683 ($\nu_{C=O}$); 1657 ($\nu_{C=O}$)
4-NO ₂	206–207	40.47	1.95	3.39	40.54	1.86	3.42	3073 (ν_{C-H}); 1717 ($\nu_{C=O}$); 1633 ($\nu_{C=O}$); 1528 (ν_{NO_2} , assym); 1329 (ν_{NO_2} , sym)

Table 2. Experimental conditions employed in the kinetic studies

Experimental variable	ArCO-Ibaz	ArCO-Imz ^a	ArCO-Phos
Solvent	13% (v/v) CH ₃ CN in water	10% (v/v) CH ₃ CN in water	Water
Buffer; μ (mol l ^{−1}); electrolyte to adjust μ ; pH range	<i>N</i> -methylmorpholine (NMeM); 0.2; KCl; 7.6–8.8	Imz; 0.07; KCl; 7.0–7.8	Potassium phosphate; 0.245–1.0; buffer and KCl, 7.2
X and λ employed (nm)	Reagent disappearance at: 250, CH ₃ ; H; Cl and CN; at 260, NO ₂	Reagent disappearance at: 253, CH ₃ ; 245, H; 252, Cl; 255, CN; 260, and NO ₂	Reagent disappearance at: 234 H; 262, Cl, CN and NO ₂ ; at 222, 3,5-dinitro
Starting [RCO-Nu] (mol l ^{−1})	Product formation at 303, NO ₂ (4–6) $\times 10^{-5}$	(1–3) $\times 10^{-5}$	(1–4) $\times 10^{-5}$

^a Data taken from Ref. 8b.

All kinetic runs were carried out in triplicate, under pseudo-first-order conditions. Slow reactions were initiated by injecting a solution of ArCO-Nu in anhydrous acetonitrile into the appropriate buffer solution, followed by homogenization with a hand-held micro-stirrer (Hellma, type 338.004). We verified that observed rate constants, k_{obs} , were independent of [ArCO-Nu] in the range $(1-6) \times 10^{-5} \text{ mol l}^{-1}$. Plots of $\log(A_{\infty} - A_t)$ and/or $\log(A_t - A_{\infty})$ versus time were rigorously linear over more than five half-lives and their slopes gave k_{obs} . For the same run, the relative standard deviation in k_{obs} , i.e. $(\text{standard deviation}/k_{\text{obs}}) \times 100$, was $\leq 0.2\%$; for triplicate runs, the difference between k_{obs} was $\leq 1\%$. The spectra of representative kinetic runs, recorded after reaction completion, were found to be identical with those of authentic mixtures of the expected products.

RESULTS AND DISCUSSION

The discussion is organized in the following order: first, we comment on the substituents employed and the reason for using *in situ* synthesis for ArCO-Phos; second, we discuss mechanistic details of the reactions of ArCO-Iba and ArCO-Phos; finally, we compare the data of these two intermediates with those of ArCO-Imz, with the objective of acquiring a better understanding of the factors controlling their reactions (Fig. 1).

Choice of the substituents and *in situ* synthesis of ArCO-Phos

The acyl group of ArCO-Iba was either benzoyl or 4-substituted benzoyl. Because the reaction of ArCO-Phos is slow, the lowest reaction temperature employed was 35°C , and we also included the 3,5-dinitrobenzoyl group. We attempted the synthesis of 4-nitrobenzoyl phosphate by reaction of the appropriate acyl chloride with lithium phosphate in dry acetonitrile and also by phase-transfer catalysis, as given for ArCO-Iba. Although the targeted mixed anhydride was obtained by the latter procedure, we did not pursue this approach because of the very low yield obtained, ca 5% for $\text{X} = \text{NO}_2$. This is probably because of the unfavorable phase transfer of the phosphate dianion.¹⁷ The above-mentioned IR data (see Experimental) show that the *in situ* procedure led to complete formation of the acyl phosphoric mixed anhydride. Additionally, we compared the rate constants for the hydrolysis of three mixed anhydrides with literature values (where the mixed anhydrides were also synthesized *in situ*), at 39°C .^{5b} The following results were obtained for $10^5 k_{\text{obs}} (\text{s}^{-1})$: 1.0, 46.7, 250^{5b} and 0.52, 41.5 and 243.3 (present study) for 4-chloro-, 4-nitro- and 3,5-dinitrobenzoyl phosphate, respectively. We attribute the differences between the two sets of data to the availability of better instrumentation at our disposal. Whereas we calculated k_{obs} by non-linear

regression of a large number of experimental points (≥ 80), their literature counterparts were based on 'five to ten points'.^{5b} In summary, *in situ* preparation of ArCO-Phos has been successfully achieved; the kinetic data obtained, k_{obs} , activation parameters and ρ , are reliable.

Hydrolysis of ArCO-Iba

Consider the hydrolysis of ArCO-Nu in the presence of Nu-NuH buffer. Catalysis by the latter, if it occurs, cannot be nucleophilic since the catalyst and the leaving group are the same. Detection of a GB catalytic pathway involves hydrolysis of ArCO-Iba in the presence of Iba-IbaH buffer. We were unable, however, to carry out this experiment because the buffer absorbs strongly in the same UV-visible region of ArCO-Iba (note that $[\text{buffer}] \gg [\text{substrate}]$). Therefore, we investigated the reaction in *N*-methylmorpholine (NMeM) buffer, whose $\text{p}K_{\text{a}}$, 7.38, is close to that of Iba. We found that k_{obs} ($0.065 \pm 0.002 \text{ s}^{-1}$) did not change as a function of increasing buffer concentration ($\text{X} = \text{CH}_3$, $T = 25^\circ\text{C}$, $[\text{NMeM}] = 0.02-0.22 \text{ mol l}^{-1}$, pH 7.8). This result indicates the absence of GB catalysis, a conclusion corroborated by the following experiment: hydrolysis of ArCO-Iba ($\text{X} = \text{CN}$) was studied at a constant concentration of NMeM (0.05 mol l^{-1} , pH 7.8), as a function of increasing the concentration of Iba (employed as a reagent). The rate constants calculated were $10^2 k_{\text{obs}} (\text{s}^{-1}) = 6.9 \pm 0.2$, 7.0 ± 0.2 , 7.5 ± 0.4 , 7.3 ± 0.3 , 7.4 ± 0.3 for the reaction in buffer solutions in the absence and in the presence of $(6, 9, 12 \text{ and } 15) \times 10^{-5} \text{ mol l}^{-1}$ Iba, respectively. The uncertainties in these rate constants are relatively large, most certainly because of the high initial absorbance (of Iba plus ArCO-Iba), coupled with the small variation of absorbance during the reaction (disappearance of the intermediate and liberation of Iba). The rate constants calculated show, however, no significant dependence on the concentration of Iba. In summary, hydrolysis of ArCO-Iba is not subject to measurable GB catalysis (by NMeM or Iba), and may proceed by solvolytic and specific base-catalyzed pathways.

Rate constants of the OH^- -catalyzed hydrolysis of ArCO-Iba were determined in the pH range 7.6–8.8 in the presence of 0.05 mol l^{-1} NMeM buffer in the temperature range $18-45^\circ\text{C}$. Table 3 shows the catalytic rate constants, k_{OH} (obtained from the slopes of the plots of k_{obs} versus $[\text{OH}^-]$) along with the corresponding activation parameters and Hammett ρ values. An experiment in D_2O ($\text{X} = \text{NO}_2$; $\text{pD} = 8.0-9.2$) indicated that $k_{\text{OD}}/k_{\text{OH}} = 0.92$.

In principle, it should be possible to determine the rate constant of the water reaction, $k_{\text{H}_2\text{O}}$, from the intercepts of the plots of k_{obs} versus $[\text{OH}^-]$. Depending on the relative magnitudes of the slope and intercept, the rate constants calculated by this procedure may be subject to relatively large uncertainties. We found, however, that the

Table 3. Catalytic rate constants and activation parameters for the OH[−]-catalyzed hydrolysis of ArCO-Iba, k_{OH} , at different temperatures and the corresponding Hammett ρ values^a

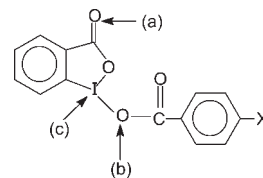
Temperature (°C)	$10^{-3}k_{\text{OH}}$ (l mol ^{−1} s ^{−1}) ^b					ρ^c
	CH ₃	H	Cl	CN	NO ₂	
18	3.06	4.76	5.95	19.02	22.01	0.92
25	6.22	10.51	13.56	42.20	46.04	0.92
35	17.67	27.14	36.43	119.28	133.31	0.95
45	40.49	68.05	88.21	279.54	325.16	0.95
Activation parameters^d						
ΔH^\ddagger (kcal mol ^{−1})	17.2	17.4	17.7	17.8	17.9	
ΔS^\ddagger (cal K ^{−1} mol ^{−1})	16.5	18.2	19.7	22.2	22.8	
ΔG^\ddagger (kcal mol ^{−1})	12.3	12.0	11.8	11.2	11.1	

^a See Experimental for the uncertainty in these rate constants.^b The following hydroxide ion concentrations were employed (10⁷ [OH[−]], X): 5.81–37.7, CH₃; 4.93–53.6, H; 5.48–58.9, Cl; 3.75–40.6, CN; 4.95–50.1, NO₂.^c The uncertainty in ρ is ≤ 0.06 .^d The uncertainties in the activation parameters are ± 0.1 kcal mol^{−1} (ΔH^\ddagger and ΔG^\ddagger) and ± 0.5 cal K^{−1} mol^{−1} (ΔS^\ddagger). In this and subsequent tables, ΔS^\ddagger is that calculated at 25 °C.**Table 4.** Second-order rate constants and activation parameters for the uncatalyzed water hydrolysis of ArCO-Iba, $k_{\text{H}_2\text{O}}$, at different temperatures and the corresponding Hammett ρ values^a

Temperature (°C)	$10^4k_{\text{H}_2\text{O}}$ (l mol ^{−1} s ^{−1})					ρ^c
	CH ₃	H	Cl	CN	NO ₂	
18	7.35	6.52	5.52	4.33	4.03	−0.26
25	13.7	13.1	10.8	9.08	8.42	−0.23
35	33.3	32.1	27.5	21.9	19.8	−0.24
45	81.8	77.3	67.5	58.0	54.3	−0.19
Activation parameters^b						
ΔH^\ddagger (kcal mol ^{−1})	15.8	16.2	16.5	16.9	16.9	
ΔS^\ddagger (cal K ^{−1} mol ^{−1})	−18.5	−17.4	−16.8	−15.8	−16.0	
ΔG^\ddagger (kcal mol ^{−1})	21.3	21.4	21.5	21.6	21.7	

^a See Experimental for the uncertainty in these rate constants. In this and subsequent tables, Ar = X-C₆H₄- and/or X₂-C₆H₃-; X = 4-Me, H, 4-Cl, 4-CN, 4-NO₂ and X₂ = 3,5-dinitro.^b The uncertainties in the activation parameters are ± 0.1 kcal mol^{−1} (ΔH^\ddagger and ΔG^\ddagger) and ± 0.5 cal K^{−1} mol^{−1} (ΔS^\ddagger).^c The uncertainty in ρ is ≤ 0.02 .

hydrolysis reaction is independent of pH in the range 0.9–4.3, and determined $k_{\text{H}_2\text{O}}$ directly, by carrying out the reaction at pH 2.80 (adjusted with HCl, $\mu = 0.2$, KCl). Table 4 shows the rate constants calculated, along with the corresponding activation parameters and Hammett ρ . Experiments in D₂O, at $\mu = 0.2$ and pD = 3.21 (= pH + 0.41),¹⁸ showed small, positive KSIE of 1.2 and 1.3 for X = CH₃ and NO₂, respectively.

**Figure 3.** Possible sites of attack on ArCO-Iba

Regarding mechanistic details of this reaction, we address the following questions.

Detection of an intermediate during hydrolysis.

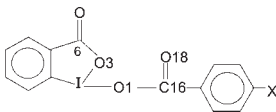
Experiments were carried out with ArCO-Iba (X = NO₂) in 50% aqueous acetonitrile, at 'nominal' pH = 7.8 (0.05 mol l^{−1} NMeM). The reason for changing the solvent composition was to slow the reaction, so that it can be conveniently monitored with a UV–visible spectrophotometer. In one experiment, the spectra of the reaction were recorded as a function of time. A sharp isosbestic point was observed at 288 nm. The hydrolysis rate constant was also determined by following the disappearance of the reactant at 260 nm and/or the appearance of the products at 303 nm. The rate constants calculated were in close agreement, 0.0113 and 0.0110 s^{−1}, respectively. Both experiments indicate either a concerted mechanism or a putative one without accumulation of a detectable intermediate.

Site of reagent (water and/or OH[−]) attack on ArCO-Iba.

As shown in Fig. 3, there are, in principle, three possible sites of attack on ArCO-Iba: (a) the C=O group of the heterocyclic ring; (b) at the C=O group of the acyl group; (c) at the iodine atom of the heterocyclic ring. Possibility (a) can easily be ruled out, since the hydrolysis reaction should be negligibly dependent on the nature of X, at variance with the results of Table 3. *Ab initio* calculations on model compounds for Iba have shown that the partial positive charge on the iodine atom is larger than the corresponding one on the carbon atom of the C=O group of the heterocyclic ring.^{11b} Our PM3 semi-empirical calculations (Table 5) on Iba and on ArCO-Iba show (at least qualitatively) that the partial positive charge on the iodine atom is larger than the corresponding ones on the carbon atoms of the C=O group of the heterocyclic ring and/or the acyl moiety. Finally, results of the following experiments show that the attack of nucleophiles on derivatives of Iba occurs at the iodine atom, as shown in Fig. 4.^{11a,c}

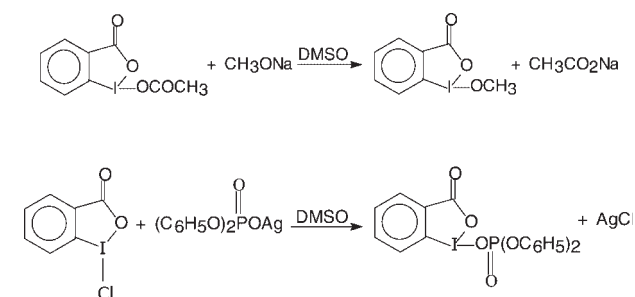
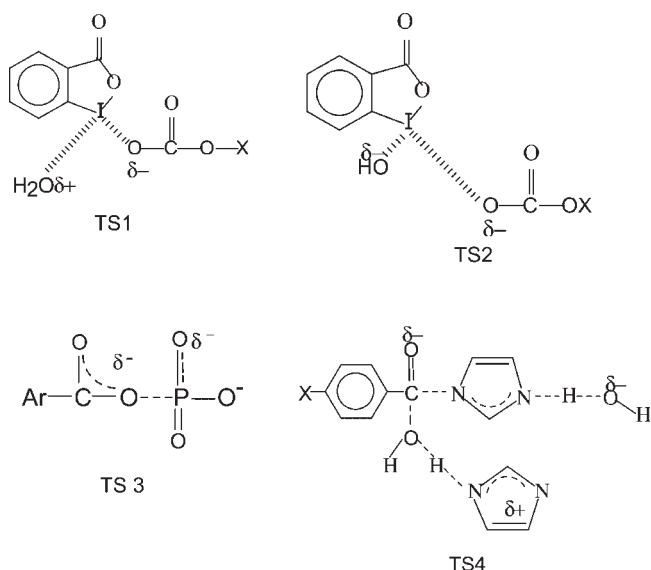
Structure of the transition state (TS) of the hydrolysis reaction.

We suggest structures TS1 and TS2 (Fig. 5) for the transition states of uncatalyzed, and OH[−]-mediated hydrolysis of ArCO-Iba, respectively. For simplicity, we only show the species that is directly attacking the iodine atom. Other solvent molecules are most certainly involved. For example, proton inventory studies of several water-catalyzed hydrolyses have shown that the attack of the 'nucleophilic' water molecule is

Table 5. Partial charges on selected atoms of Iba, acetyl-Iba and ArCO-Iba, calculated by the PM3 semi-empirical method


Compound	Atom					
	I	O3	O1	O18	C6	C16
Iba	0.8248	-0.4574	-0.8718	—	0.6117	—
ArCO-Iba						
Me	0.8457	-0.4690	-0.6816	-0.5870	0.6118	0.6796
H	0.8464	-0.4678	-0.6812	-0.5852	0.6116	0.6781
Cl	0.8474	-0.4663	-0.6808	-0.5830	0.6114	0.6752
CN	0.8492	-0.4620	-0.6800	-0.5750	0.6103	0.6701
NO ₂	0.8510	-0.4585	-0.6799	-0.5721	0.6094	0.6672
CH ₃ CO-Iba ^a	0.8531	-0.3969	-0.6816	-0.5804	0.6078	0.6275

^a The atom numbering for CH₃CO-Iba is the same as that for ArCO-Iba.

**Figure 4.** Mechanism of attack of nucleophiles on derivatives of Iba**Figure 5.** Suggested structures for the transition states of attack of water (TS1) and OH⁻-mediated reaction of ArCO-Iba (TS2), spontaneous decomposition of ArCO-Phos (TS3), and GB-catalyzed hydrolysis of ArCO-Imz, TS4

usually catalyzed by one or more 'GB' water molecules.^{7d,e,18} Additionally, the hydroxide ion is known to be strongly solvated by several water molecules.¹⁹ Our suggestion is based on the data in Tables 3–5 and the

following reasoning. (i) Since the TSs are more polar than the precursor organic substrates, ρ essentially reflects the effects of X (stabilization/destabilization) on the charges that are being developed on the reaction center. For the water reaction ρ is close to zero, whereas $\rho = 0.92$ for the OH⁻-mediated hydrolysis (at 25 °C). Both results reflect the attenuated transmission of the electronic effects of X to the iodine atom in TS1 and TS2. One measure of this attenuation is the slope of plot of partial charge on the atom of concern (Table 5) versus σ_X , 0.0051 and -0.0128, for the iodine atom and the acyl carbon atom, respectively. Therefore, the electronic effects of X are transmitted to the iodine atom less efficiently than to the carbon atom of the acyl group, which decreases $|\rho|$. Additionally, the smaller degree of charge development in TS1 further decreases $|\rho|$. (ii) The TSs suggested also agree with the entropies of activation and the KSIE. The water reaction is associated with a negative ΔS^\ddagger and a relatively small but positive KSIE (i.e., $k_{H_2O} > k_{D_2O}$). Negative ΔS^\ddagger are expected for bimolecular reactions involving ArCO-Iba and one or more water molecules, but the magnitude of KSIE (≤ 1.3) is smaller than that expected for a typical water-catalyzed reaction (> 2.0).^{7d,e,18} The small KSIE may be the consequence of the reactant-like structure of TS1, with little bond formation and bond breaking. Alternatively, the reaction coordinate might be dominated by the movement of heavy atoms, especially the oxygen, with subordinate proton transfer, characterized by a low amplitude of motion at the TS. This mode of GB catalysis (e.g. by a second water molecule) may be associated with a small KSIE.²⁰

The OH⁻-mediated reaction is associated with *positive* ΔS^\ddagger , inverse KSIE ($k_{OH} < k_{OD}$), and ρ that is lower than the range reported for acyl-transfer reactions of substituted benzoates ($\rho \geq 1.2$). TS2 shows more bond formation and breaking than TS1. Therefore, the sign of ρ is expected, since an electron-withdrawing group should favor both the formation of the OH⁻-iodine bond and the

breaking of the iodine–carboxylate group bond. The positive ΔS^\ddagger is interesting because negative values are expected for bimolecular reactions, provided that the reaction is controlled by its intrinsic energy barrier, i.e. that due to bond breaking and formation. However, for reactions involving a neutral molecule and a strongly solvated species, in particular the alkoxide and hydroxide ions, the energetics may be partially or completely dominated by the desolvation barrier, i.e. that required to desolvate the base, with concomitant introduction of the neutral reagent into its solvation microsphere.²¹ Therefore, the positive entropy of activation seems to be due to the increase in the degree of freedom of the water molecules, liberated by the (partial) desolvation of the hydroxide ion. In this regard, it is relevant that several bimolecular reactions are accompanied with positive entropies of activation.²² Additionally, in OH^- -mediated reactions, the H/D fractionation factor of the attacking OH^- usually increases on going from the reactant state, RS, to the TS.^{18,20} This increase reflects the diminished role of the solvent shell on covalent bond formation between oxygen and iodine, in agreement with a positive entropy of activation. Finally, there is reason to expect an inverse KSIE since OD^- is a stronger base than OH^- .

Breakdown of ArCO-Phos

Reactions of acyl phosphates have been studied in some detail, including the hydrolysis of acetyl phosphate, and of some benzoyl phosphates at a single temperature, 39 °C, in the pH range 6.9–7.5.^{5b} In the present study, the rate constants were determined more accurately and the activation parameters were calculated and are discussed in terms of reaction mechanism. The pK_a values of 4-methoxybenzoyl-, 4-nitrobenzoyl- and 3,5-dinitrobenzoyl phosphate were estimated as 4.8, 4.3 and 4.0, respectively.^{5b} Therefore, at the pH employed in the present study, 7.2, *all our kinetic data refer to the reaction of ArCO-Phos dianion*. The following results show that the rate of reaction of 3,5-dinitrobenzoyl phosphate is insensitive to the variation of buffer concentration ($\mu = 0.78 \text{ mol l}^{-1}$; pH = 7.20; $T = 39^\circ\text{C}$); $[\text{HPO}_4^{2-}] = 0.1, 0.2, 0.3 \text{ mol l}^{-1}$; $k_\text{obs} = 0.0260 \pm 0.001$; 0.0256 ± 0.001 ; $0.0250 \pm 0.001 \text{ s}^{-1}$, respectively. Under the same reaction conditions, using 0.1 mol l^{-1} phosphate buffer, the reaction was found to be independent of pH in the range 6–8; there was only a 5.4% rate constant increase when μ was increased (KCl) from 0.245 to 1.0 mol l^{-1} ; and a 2.5% decrease in k_obs when the solvent was changed from H_2O to D_2O . These data agree with those observed for the hydrolysis of acetyl phosphate dianion, which indicated that the reaction is not subject to specific-base and/or GB catalysis, and that water does not participate in the slow step of hydrolysis.^{5b} The latter conclusion means that the activation parameters should

Table 6. Rate constants and activation parameters for the spontaneous breakdown of ArCO-Phos, k_spont , at different temperatures and the corresponding Hammett ρ values^a

Temperature (°C)	$10^5 k_\text{spont} (\text{s}^{-1})$					ρ^c
	H	Cl	CN	NO_2	Dinitro	
35	1.2	2.8	15.2	24.2	144.6	1.48
45	6.9	14.8	68.2	91.7	509.0	1.32
50	16.2	33.1	139.7	173.2	927.7	1.24
55	37.0	72.0	279.9	320.7	1659.9	1.16
<i>Activation parameters^b</i>						
ΔH^\ddagger (kcal mol^{-1})	33.8	32.0	28.7	25.4	23.9	
ΔS^\ddagger ($\text{cal K}^{-1} \text{mol}^{-1}$)	28.7	24.5	17.0	7.2	6.1	
ΔG^\ddagger (kcal mol^{-1})	25.3	24.7	23.6	23.2	22.1	

^a See Experimental for the uncertainty in these rate constants.

^b The uncertainties in the activation parameters calculated at 25 °C are $\pm 0.1 \text{ kcal mol}^{-1}$ (ΔH^\ddagger and ΔG^\ddagger) and $\pm 0.5 \text{ cal K}^{-1} \text{mol}^{-1}$ (ΔS^\ddagger).

^c The uncertainty in ρ is ≤ 0.08 .

be calculated from k_obs (not $k_\text{obs}/[\text{water}]$), a point of conflict in the literature.^{5b,23} Table 6 shows the rate constants for the spontaneous decomposition of ArCO-Phos, along with the corresponding Hammett ρ values and the activation parameters.

In agreement with these data, and with previous results, we propose TS3 (Fig. 5) for the spontaneous decomposition of ArCO-Phos. This TS structure agrees with the positive ΔS^\ddagger because the degrees of freedom increase on going from RS to TS. Note that several solvation/desolvation interactions contribute to ΔS^\ddagger , and may cancel out partially, including desolvation of the reactant, and solvation of the produced benzoate and metaphosphate anions (the latter rapidly hydrolyzes to phosphate). Since there is no nucleophilic addition of water to ArCO-Phos, the practically unity of KSIE is not unexpected. The large, positive ρ indicates a significant negative charge development in the benzoate moiety. The noticeable sensitivity of ρ to the temperature, not observed for the other ArCO-Nu, is interesting and will be considered later. Finally TS4 is that suggested for the GB-catalyzed hydrolysis of ArCO-Imz.

Comparison of the reactions of RCO-Iba, RCO-Imz and RCO-Phos

We now compare the data obtained under experimentally similar conditions (Table 7) for the reactions of the three species, ArCO-Imz, ArCO-Iba and ArCO-Phos, which occur via the different mechanisms depicted in Fig. 1. In what follows, we are always concerned with the changes that occur between the reactant state, RS, and the TS. For

Table 7. Kinetic criteria for the mechanisms of reactions of ArCO-Nu^a

Parameter	ArCO-Imz			ArCO-Iba ^d		ArCO-Phos ^d
	k_{GB}^b	$k_{H_2O}^c$	k_{OH}^c	k_{H_2O}	k_{OH}	k_{spon}
KSIE	2.94	2.54	1.13	1.2	—	1.03
	2.43	2.36	1.03	1.3	0.92	0.96
ρ	1.25	1.41	1.47	−0.22	0.92	1.65
						1.2 ^e
ΔH^\ddagger (kcal mol ^{−1})	10.4	10.4	7.0	15.8	17.2	35.5
	7.9 ^b	12.1	12.0	17.1	18.1	25.4
						26.6 ^f
ΔS^\ddagger (cal K ^{−1} mol ^{−1})	−36.9	−44.6	−43.4	−18.7	16.5	33.0
	−40.0	−32.7	−20.3	−15.2	22.6	7.2
						3.7 ^f
ΔG^\ddagger (kcal mol ^{−1})	21.4	23.7	19.9	21.3	12.3	25.8
	19.8	21.8	18.1	21.6	11.1	23.2
						25.4 ^f
ΔH^\ddagger versus σ^g	−2.6	1.8	−0.4	1.2	0.7	−9.9
ΔS^\ddagger versus σ^g	−2.8	12.6	−4.8	3.1	6.4	−24.6

^a In each column, the upper and lower figures refer to X = 4-CH₃ and 4-NO₂, respectively. All data are at 25 °C.

^b Data taken from Ref. 8b.

^c The data for k_{H_2O} and k_{OH} were taken from Ref. 7b and 7c. Where needed, the Hammett equation was employed in order to calculate the required rate constant.

^d Data from the present work.

^e Data for ArCO-Phos at 39 °C, from Ref. 5b.

^f Data for acetyl phosphate, from Ref. 5b.

^g These are the slopes of plots of the appropriate activation parameters of ArCO-Nu versus Hammett σ of the substituents.

brevity, we employ the terms benzoate and Iba anions to indicate the corresponding *incipient anions* in the TS. Additionally, ArCO-Phos refers to the acyl phosphate dianion. The substituent effects on ΔH^\ddagger and ΔS^\ddagger are listed in the last two rows of Table 7 and correspond to the slopes of the (reasonably linear) dependence of these parameters on σ_X . For comparison, we also include published data for the following reaction paths: k_{H_2O} and k_{OH} for ArCO-Imz and k_{spon} for acetyl phosphate dianion. The following points are relevant:

1. The relationship between ρ and the catalytic pathway is not straightforward. Therefore, the usefulness of this parameter in understanding the pathway-determining factors of these reactions is limited. However, all ρ clearly indicate a moderate to large charge development in the benzoate moiety of the TSs.
2. The dependence of KSIE and of ΔS^\ddagger on the mechanism is clear. That is, water attack, when catalyzed by a GB (either another water molecule and/or the buffer) is associated with a large KSIE and highly negative entropy of activation. In contrast, the decomposition of ArCO-Phos is associated with a negligible KSIE and positive ΔS^\ddagger since its slow step does not involve water. The less than expected KSIE for k_{H_2O} of ArCO-Iba has been discussed.
3. More interestingly, the activation parameters, ΔH^\ddagger and ΔS^\ddagger , are substituent dependent, as shown in the last two rows of Table 7. Except for one case, k_{GB} of ArCO-Imz, the |slope| of the ΔS^\ddagger versus σ_X plot is much larger the corresponding value for ΔH^\ddagger . Therefore, changes in solvation of the relevant species, the

hydroxide ion (for k_{OH} pathway) and the leaving benzoate and Iba anions play an important role in the reactivity of the ArCO-Nu investigated. As the ΔS^\ddagger versus σ_X plots clearly indicate, changes in the solvation of the benzoate anion is substituent dependent since the developing negative charge is competitively stabilized by the solvent and by the substituent X. Accordingly, electron-withdrawing substituents are expected to stabilize the benzoate anion and decrease its solvation. We now examine how this interpretation applies to the data for the above-discussed reaction pathways.

4. First we consider the OH[−]-mediated reactions of ArCO-Imz and ArCO-Iba. In these cases, there is no change in the overall charge but a large charge reorganization, leading to changes in solvation. Since the charge on the OH[−] decreases, its solvation decreases and the corresponding contribution to ΔS^\ddagger is expected to be positive. On the other hand, the charges on the forming benzoate and/or Iba anions increase, leading to an increase in solvation and a corresponding decrease in ΔS^\ddagger . The results obtained (magnitude of ΔS^\ddagger and its dependence on σ_X) indicate that the balance between the two opposite effects is different for the above-mentioned substrates. For ArCO-Imz, ΔS^\ddagger is highly negative and exhibits a small dependence on σ_X . This indicates little desolvation of the entering OH[−] associated with a small solvation of the leaving benzoate. In contrast, the same pathway for ArCO-Iba is associated with positive ΔS^\ddagger and high dependence on the substituent. Both results indicate extensive OH[−] desolvation, which more than

counterbalances the effects on ΔS^\ddagger of the solvation of the benzoate and Iba anions. Note that attack of nucleophiles on the Iba moiety is unhindered since the I—O bond protrudes almost linearly (the O—I—O angle is 165°), ca 2 Å from the heterocyclic ring.²⁴

5. Some uncatalyzed water reactions involve large charge development, therefore ΔS^\ddagger is expected to be negative and substituent dependent. This is clearly the case for the $k_{\text{H}_2\text{O}}$ pathway of ArCO-Imz. For the ArCO-Iba, ΔS^\ddagger is negative, although less dependent on X, relative to *N*-benzoylimidazole. This essentially reflects the smaller degree of charge development on the benzoate anion, as indicated by the negligible $|\rho|$ of this reaction.
6. The unimolecular reaction of ArCO-Phos behaves differently from the bimolecular reactions, e.g. all ΔS^\ddagger values are positive and decrease on going from X = 4-methyl to 4-nitro. This is contrary to what is expected, based on the effects of X on solvation of the benzoate anion (see above). Additionally, the associated substituent effect on ΔH^\ddagger is not as negligible as those on the above-discussed bimolecular reactions. As recently argued^{10e} for monophosphate ester dianions, e.g. $4\text{-XC}_6\text{H}_4\text{O-PO}_3^{2-}$, the interaction of an electron-withdrawing X with the bridging oxygen leads to slight stretching of the bridging O—P bond. In the TS, this bond is nearly broken, i.e. the interaction energy with X is expected to be much stronger than in the RS. Therefore, relative to an electron-releasing X, there is more charge dispersion in the RS and an extensive one in the TS when X is electron withdrawing, in agreement with the very large dependence of ΔS^\ddagger on σ_X . The positive entropy is a consequence of these differences in solvation and the dissociative nature of the TS.

CONCLUSIONS

The mechanism of reactions of ArCO-Nu is strongly dependent on the nucleophile and the nature of ArCO. For example, the OH^- -mediated reactions of ArCO-Iba and ArCO-Imz exhibit very different features. At 25°C , ρ for ArCO-Iba (0.92) is markedly smaller than that for ArCO-Imz (1.47), in agreement with different sites of nucleophilic attack: iodine atom and benzoyl carbon atom, respectively. More surprisingly, the calculated ΔS^\ddagger are moderately positive and significantly substituent dependent in the reaction of ArCO-Iba and highly negative and much less dependent on σ for ArCO-Imz. These entropy data are interpreted in terms of a balance between OH desolvation and solvation of the forming benzoate and/or Iba in the TS. Whereas these two opposite effects are large for ArCO-Iba, they do not play an important role in case of ArCO-Imz, probably because of the very different requirements of solvation of (neutral) Imz and (anionic) Iba. Analogous conclusions

can be drawn for the $k_{\text{H}_2\text{O}}$ path of the same two ArCO-Nu. In particular, the sites of nucleophilic attack on ArCO-Iba and ArCO-Imz are different, which leads to very different ρ values. Regarding the spontaneous decomposition of ArCO-Phos we have shown, for the first time, that the highly positive activation entropy decreases noticeably when X is electron withdrawing. We interpreted our result not only in terms of reactant desolvation (a dianion) but also of the Hammond postulate, i.e. electron-withdrawing X induce earlier TSs. Therefore, the previous assumption on the large solvation requirements of the phosphate reactions, mainly based on the data for a single compound (e.g. an acyl phosphate or a phosphate ester), should be revised since our results indicate little solvation when X is strongly electron withdrawing. In conclusion, our data and, in particular, those on the substituent dependence of the activation parameters shed light on the importance of solvation in reactions of biochemical interest.

Acknowledgments

We thank the São Paulo State Research Foundation, FAPESP, for financial support, and the National Research Council, CNPq, for research fellowships to W. A. Rodrigues and M. Ferreira and a research productivity fellowship to O. A. El Seoud. This work was carried out within a CAPES/COFECUB bilateral cooperation project.

REFERENCES

1. Bender ML, Bergeron RJ, Komiyama M. *The Bioorganic Chemistry of Enzyme Catalysis*. Plenum Press: New York, 1984; 45.
2. Jencks WP. *Catalysis in Chemistry and Enzymology*. Dover: New York, 1987; 42, 463.
3. Isaacs NS. *Physical Organic Chemistry*. Longman: Harlow, 1987; 375.
4. Carry FA, Richard JS. *Advanced Organic Chemistry, Part A* (4th edn). Kluwer: New York, 2000; 449.
5. (a) Jencks WP, Carriuolo J. *J. Am. Chem. Soc.* 1961; **83**: 1743–1750; (b) Di Sabato G, Jencks WP. *J. Am. Chem. Soc.* 1961; **83**: 4400–4405; (c) Kirby AJ, Jencks WP. *J. Am. Chem. Soc.* 1965; **87**: 3209–3216, 3217–3224; (d) O'Connor CJ, Wallace RG. *Aust. J. Chem.* 1984; **37**: 2559–2569; (e) Herschlag D, Jencks WP. *Aust. J. Chem.* 1989; **111**: 7579–7587; (f) Herschlag D, Jencks WP. *Aust. J. Chem.* 1990; **112**: 1942–1950.
6. (a) Hubbard CD, Kirsch JF. *Biochemistry* 1972; **11**: 2483–2493; (b) Castro EA, Steinfort GB. *J. Chem. Soc., Perkin Trans. 2* 1983; 453–457.
7. (a) Klinmann JP, Thornton ER. *J. Am. Chem. Soc.* 1968; **90**: 4390–4394; (b) Choi M-U, Thornton ER. *J. Am. Chem. Soc.* 1974; **96**: 1428–1436; (c) Palaitis W, Thornton EER. *J. Am. Chem. Soc.* 1975; **97**: 1193–1196; (d) Gopalakrishnan G, Hogg JI. *J. Org. Chem.* 1983; **48**: 2038–2043; (e) Barbaro J, Gopalakrishnan G, Hogg JI. *J. Org. Chem.* 1989; **54**: 4438–4443.
8. (a) Menegheli P, Farah JPS, El Seoud OA. *Ber. Bunsenges. Phys. Chem.* 1991; **95**: 1610–1615; (b) El Seoud OA, Menegheli P, Pires PAR, Kiyani NZ. *J. Phys. Org. Chem.* 1994; **7**: 431–437; (c) El Seoud OA, Martins MF. *J. Phys. Org. Chem.* 1995; **8**: 637–646; (d) El Seoud OA, Ruasse M-F, Rodrigues WA. *J. Chem. Soc., Perkin Trans. 2* 2002; 1053–1058.

9. (a) Benkovic SJ, Schray KJ. In *Transition States of Biochemical Processes*, Gandour RD, Schowen RL (eds). Plenum Press: New York, 1978; 493; (b) Williams A. *Acc. Chem. Res.* 1989; **22**: 387–392; (c) Thatcher GRJ, Kluger R. *Adv. Phys. Org. Chem.* 1989; **25**: 99–265; (d) Castro EA. *Chem. Rev.* 1999; **99**: 3505–3524.
10. (a) Hollfelder F, Herschlag D. *Biochemistry* 1995; **34**: 12255–12264; (b) Admiraal SJ, Herschlag D. *J. Am. Chem. Soc.* 1999; **121**: 5837–5845; (c) Admiraal SJ, Herschlag D. *J. Am. Chem. Soc.* 2000; **122**: 2146–2148; (d) O'Brien PJ, Herschlag D. *Biochemistry* 2002; **41**: 3207–3225; (e) Cheng H, Nikolic-Hughes I, Wang JH, Deng H, O'Brien PJ, Wu L, Zhang Z-Y, Herschlag D, Callender R. *J. Am. Chem. Soc.* 2002; **124**: 11295–11306.
11. (a) Mackay RA, Longo FR, Knier BL, Durst HD. *J. Phys. Chem.* 1987; **91**: 861–864; (b) Moss RA, Scrimin P, Rosen RT. *Tetrahedron Lett.* 1987; **28**: 251–254; (c) Moss RA, Wilk B, Krogh-Jespersen K, Blair JT, Westbrook JD. *J. Am. Chem. Soc.* 1989; **111**: 250–258; (d) Yang Y-C, Baker JA, Ward R. *Chem. Rev.* 1992; **92**: 1729–1743; (e) Moss RA, Zhang H. *J. Am. Chem. Soc.* 1994; **116**: 4471–4472.
12. Berg FJ, Moss RA, Yang YC, Zhang HM. *Langmuir* 1995; **11**: 411–413.
13. (a) Moss RA, Morales-Rojas H, Zhang HM, Park BD. *Langmuir* 1999; **15**: 2738–2744; (b) Moss RA, Morales-Rojas H. *Langmuir* 2000; **16**: 6485–6491.
14. Perrin DD, Armarego WLF, Perrin DR. *Purification of Laboratory Chemicals* (2nd edn). Wiley-Interscience: New York, 1988.
15. (a) Saunders BC, Stacey GJ, Wilding IGE. *Biochem. J.* 1942; **36**: 368–375; (b) Ashley JN, Barber H, Oanea D, Johnson D. *J. Chem. Soc.* 1942; 103–116; (c) Weast RC (ed). *Handbook of Chemistry and Physics* (73rd edn). CRC Press: Boca Raton, FL, 1993.
16. Camici G, Manao G, Cappugi G, Ramponi G. *Experientia* 1976; **32**: 535–536.
17. Demhlow EV, Demhlow SS. *Phase Transfer Catalysis* (2nd edn). Verlag Chemie: Weinheim, 1983; 14.
18. Showen K. In *Transition States of Biochemical Processes*, Gandour RD, Schowen RL (eds). Plenum Press: New York, 1978; 225.
19. (a) Marcus Y. *Ion Solvation*. Wiley: New York, 1985; 87; (b) Krestov GA. *Thermodynamics of Solvation*. Ellis Horwood: Chichester, 1991; 97.
20. (a) Alvarez F, Schowen RL. In *Isotopes in Organic Chemistry*, Buncel E, Lee CC (eds). Elsevier: New York, 1984; 1–60; (b) Kovach IM, Bennet AJ, Bibbs JA, Zhao Q. *J. Am. Chem. Soc.* 1993; **115**: 5138–5144.
21. Dewar MJS, Storch DM. *J. Chem. Soc., Perkin Trans. 2* 1989; 877–885.
22. (a) Queen A. *Can. J. Chem.* 1967; **45**: 1619–1629; (b) Felton SM, Bruice TC. *J. Am. Chem. Soc.* 1969; **91**: 6721; (c) Buncel E, Raoult A. *Can. J. Chem.* 1972; **50**: 1907–1911; (d) Bhatt MV, Rao KS, Rao V. *J. Org. Chem.* 1977; **42**: 2697–2702.
23. Kurz JL, Gutsche CD. *J. Am. Chem. Soc.* 1960; **82**: 2175–2181.
24. Banks DF. *Chem. Rev.* 1966; **66**: 243–266.